Supplementary Information

A retinoic acid-enhanced, multicellular human blood-brain barrier model derived from stem cell sources

Ethan S. Lippmann, Abraham Al-Ahmad, Samira M. Azarin, Sean P. Palecek, and Eric V. Shusta

Inventory of Supplementary Information

Table S1. Antibodies used for flow cytometry (FC) and immunocytochemistry (ICC).

Target antigen	Antibody species	Vendor	Clone or product number	Dilution
PECAM-1	Rabbit	Thermo Scientific	RB-10333P	1:10 (FC) 1:25 (ICC)
GLUT-1	Mouse	Thermo Scientific	SPM498	1:50 (ICC&FC)
Occludin	Mouse	Life Technologies	OC-3F10	1:100 (ICC) 1:50 (FC)
Claudin-5	Mouse	Life Technologies	4C3C2	1:100 (ICC) 1:50 (FC)
VE-Cadherin	Mouse	Santa Cruz Biotechnologies	F8	1:25 (ICC) 1:500 (FC)
E-cadherin	Goat	R&D Systems	AF648	1:100 (ICC&FC)
P-glycoprotein	Mouse	Life Technologies	F4	1:25 (ICC) 1:50 (FC)
Breast cancer resistance protein (BCRP)	Mouse	Millipore	5D3	1:25 (ICC) 1:50 (FC)
Multidrug resistance protein 1 (MRP1)	Mouse	Millipore	QCRL-1	1:100 (ICC) 1:50 (FC)
Glial fibrillary acidic protein (GFAP)	Rabbit	Dako	Z0334	1:500 (ICC)
βIII tubulin	Rabbit	Sigma	T2200	1:1000 (ICC)
Nestin	Mouse	Millipore	10C2	1:500 (ICC)
α smooth muscle actin (SMA)	Mouse	American Research Products	1A4	1:100 (ICC)
Platelet-derived growth factor β (PDGFRβ)	Rabbit	Cell Signaling	28E1	1:100 (ICC)

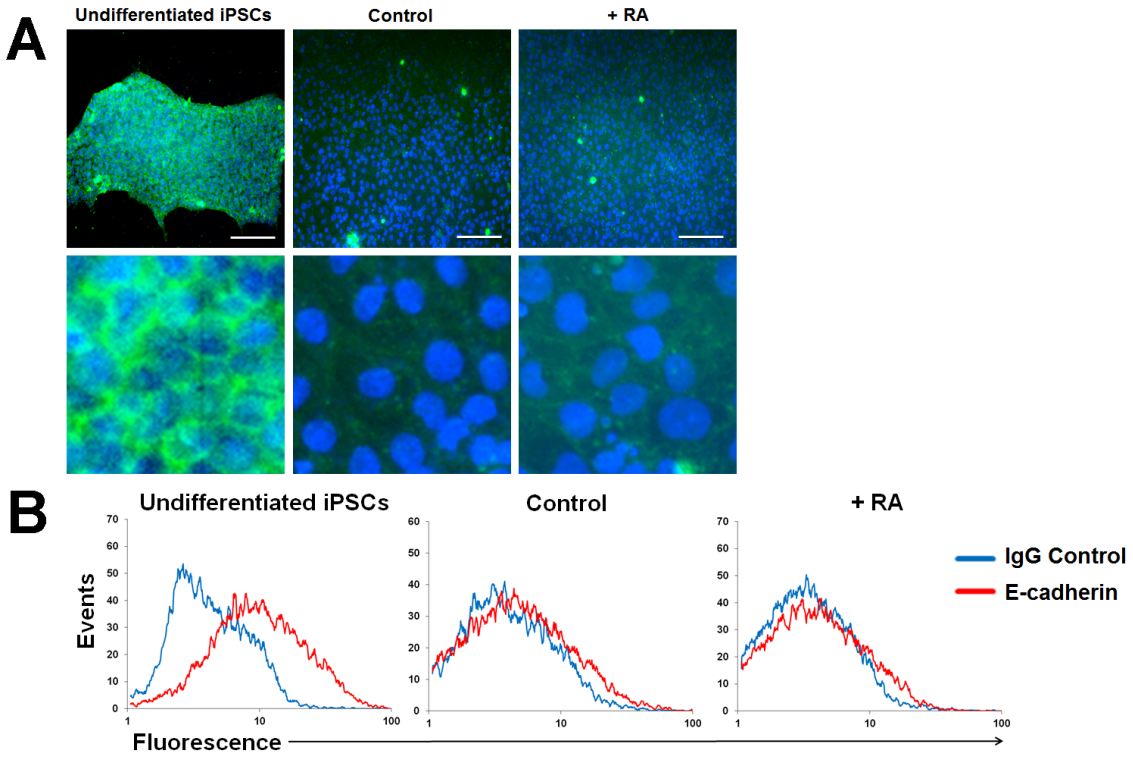

Fig. S1. Expression of E-cadherin in undifferentiated IMR90-4 iPSCs and mixed cultures after 6 days of UM treatment and 2 days of EC medium treatment with or without RA. (A) Immunolabeling for E-cadherin. DAPI overlay is shown. Scale bars on upper row, 100 μm. The lower row is a zoomed-in frame from each picture in the upper row to show junctional labeling. Exposure time was the same for each image to demonstrate strong labeling in the undifferentiated iPSCs and weak labeling after differentiation. Importantly, treatment with RA did not induce E-cadherin expression compared to control cells. (B) Flow cytometric histograms of E-cadherin at the same time points as panel A.

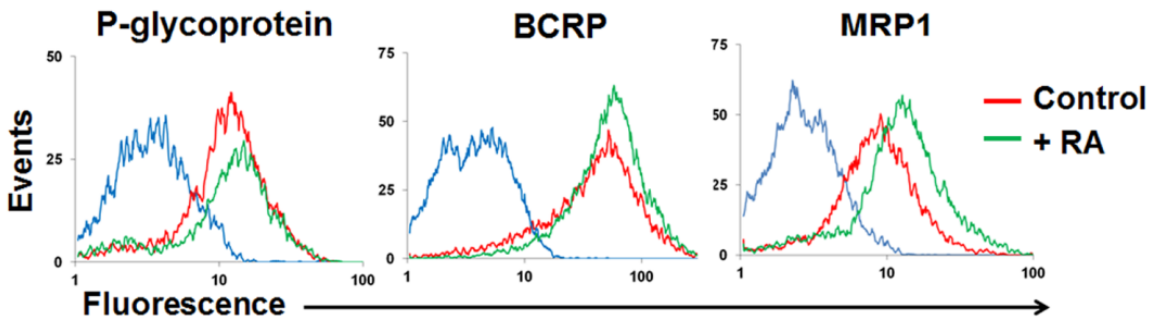

Fig. S2. Flow cytometric detection of p-glycoprotein, BCRP, and MRP1 in purified IMR90-4-derived BMECs. Blue histogram, IgG control. MRP1 exhibits 1.3-fold upregulation due to RA treatment. Results are representative of two biological replicates.

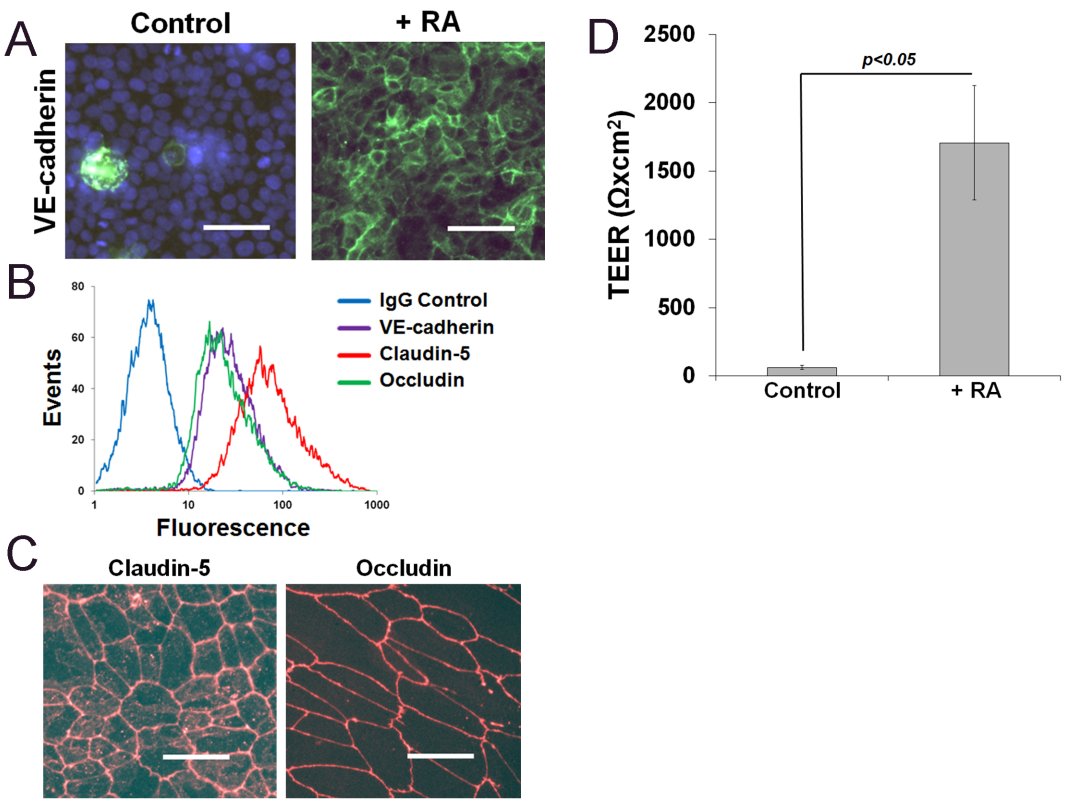

Fig. S3. RA treatment on DF-19-9-11T-derived BMECs. (A) Addition of RA during the EC medium phase induces VE-cadherin expression. DAPI is overlaid in the control image. Scale bars, 50 μm. (B) Flow cytometric analysis of BMEC purity after subculture. (C) Immunocytochemical analysis of claudin-5 and occludin tight junction protein localization. Scale bars, 50 μm. (D) RA treatment increases TEER in DF19-9-11T-derived BMECs. Mean ± S.D. was calculated from triplicate filters and statistical significance was calculated using the student's unpaired t-test.

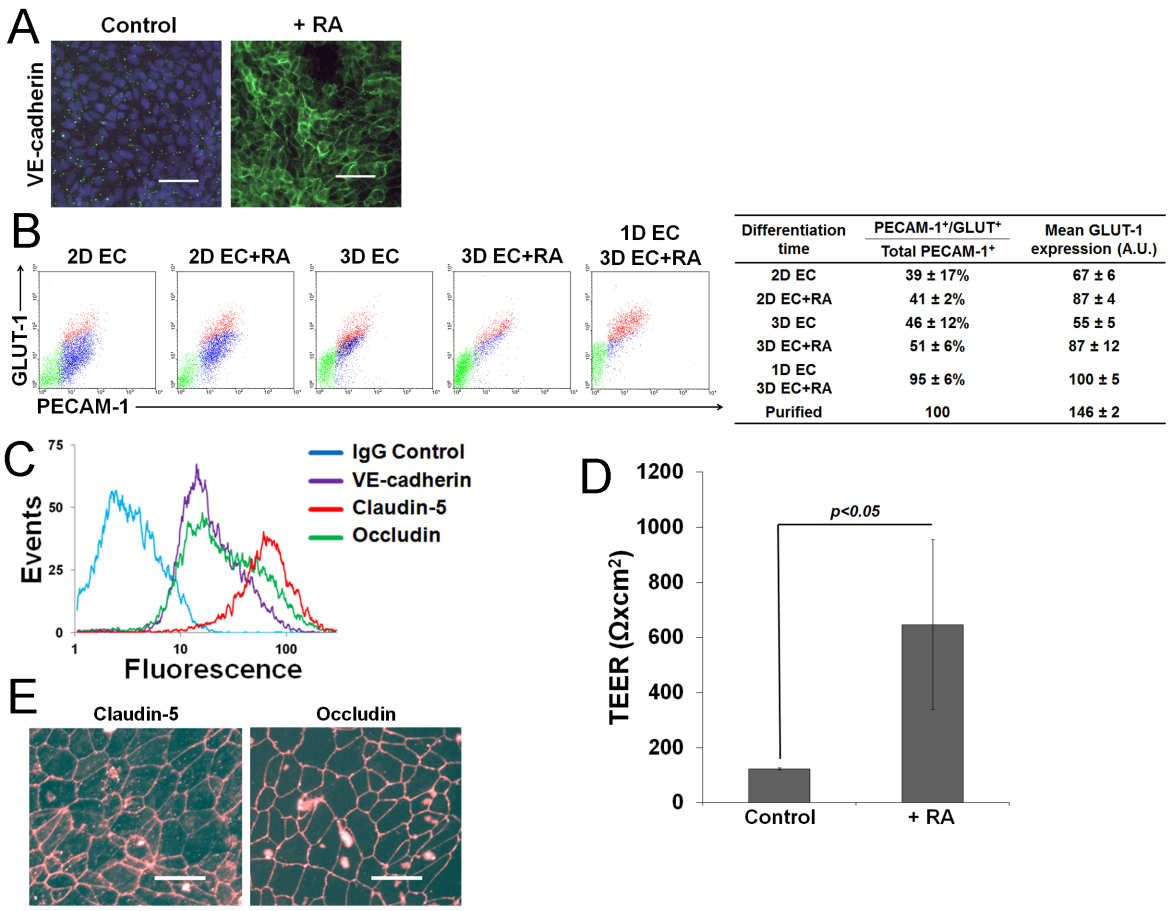

Differentiation time	PECAM-1⁺/GLUT⁺ / Total PECAM-1⁺	Mean GLUT-1 expression (A.U.)
2D EC	39 ± 17%	67 ± 6
2D EC+RA	41 ± 2%	87 ± 4
3D EC	46 ± 12%	55 ± 5
3D EC+RA	51 ± 6%	87 ± 12
1D EC 3D EC+RA	95 ± 6%	100 ± 5
Purified	100	146 ± 2

Fig. S4. RA regulates BBB properties in H9-derived BMECs. (A) Addition of RA for 48 h of the EC medium phase (6D UM 2D EC) induces VE-cadherin expression. Scale bars, 50 μm. (B) Representative dual-label flow cytometry plots for PECAM-1 and GLUT-1 during H9 hESC differentiation. All samples were differentiated in UM for 6 days prior to varying permutations of EC medium treatment. Red dots, PECAM-1$^+$/GLUT-1$^+$ cells; blue dots, PECAM-1$^+$/GLUT-1$^-$ cells; green dots, PECAM-1$^-$/GLUT-1$^-$ cells. Results are quantified and presented in the adjacent table as the percentage of PECAM-1$^+$/GLUT-1$^+$ BMECs within the overall PECAM-1$^+$ population. GLUT-1 mean expression was quantified within the PECAM-1$^+$/GLUT-1$^+$ BMEC population. Mean ± S.D. was calculated using two biological replicates for each condition. (C) Flow cytometry analysis of VE-cadherin, claudin-5, and occludin expression in purified RA-treated cells. (D) TEER values for control and RA-treated cells. Mean ± S.D. was averaged from

biological replicates (see Table 1 for full details). Statistical significance was calculated using the student's unpaired t-test. (E) Immunocytochemical analysis of tight junction fidelity in RA-treated BMECs. Scale bars, 50 μm.

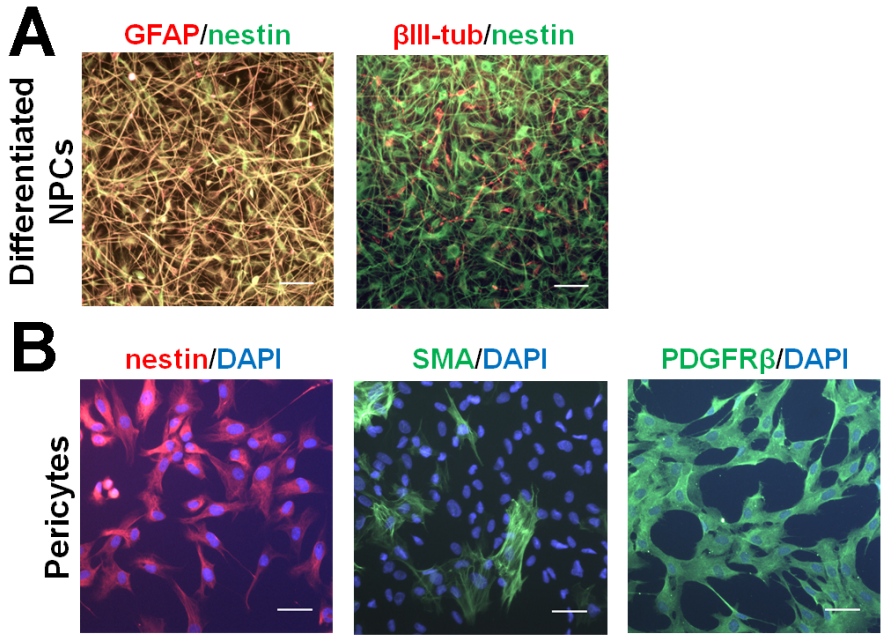

Fig. S5. Characterization of co-cultured cell populations by immunocytochemistry. (A) Immunolabeling of human NPCs differentiated for 15 days for glial fibrillary acid protein (GFAP), βIII-tubulin, and nestin. Cultures were primarily GFAP$^+$/nestin$^+$ astrocytes and βIII tubulin$^+$/nestin$^-$ neurons, similar to previous results[1]. Scale bars, 50 μm. (B) Immunolabeling of primary human fetal brain pericytes for nestin, alpha smooth muscle actin (SMA), and platelet-derived growth factor receptor beta (PDGFRβ). Pericytes in capillaries have been previously shown to express nestin and PDGFRβ whereas endothelial cells do not[2-4]. Thus, uniform expression of these proteins was expected in cultured pericytes. SMA is not expressed in capillaries (pericytes or endothelial cells) *in vivo*[2, 3], but *in vitro* exposure to factors such as serum[3, 5] or transforming growth factor β[6] can induce SMA expression. As such, the expression of SMA in these cultured pericytes is likely reflective of our use of serum-containing media. DAPI nuclear stain is overlaid in all images. Scale bars, 50 μm.

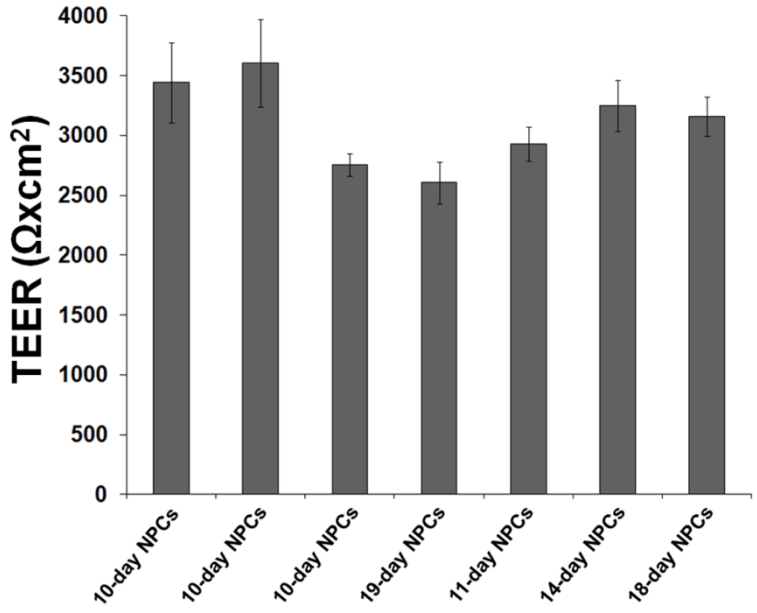

Fig. S6. TEER measured in RA-treated IMR90-4-derived BMECs under the PNPC co-culture condition in NPC medium. The number of days NPCs were differentiated prior to co-culture is indicated on the bar graph. Data are analogous to the conditions presented in Figure 3D. Each bar represents an independent biological replicate and mean ± S.D. were calculated from triplicate filters. The replicate with the highest TEER (10-day NPCs, 3,610 ± 370 Ωxcm^2) is listed in Table 2.

References

1. Lippmann, E.S., Weidenfeller, C., Svendsen, C.N. & Shusta, E.V. Blood-brain barrier modeling with co-cultured neural progenitor cell-derived astrocytes and neurons. *Journal of neurochemistry* **119**, 507-520 (2011).
2. Crisan, M. et al. A perivascular origin for mesenchymal stem cells in multiple human organs. *Cell stem cell* **3**, 301-313 (2008).
3. Dore-Duffy, P., Katychev, A., Wang, X. & Van Buren, E. CNS microvascular pericytes exhibit multipotential stem cell activity. *J Cereb Blood Flow Metab* **26**, 613-624 (2006).
4. Daneman, R., Zhou, L., Kebede, A.A. & Barres, B.A. Pericytes are required for blood-brain barrier integrity during embryogenesis. *Nature* **468**, 562-566 (2010).
5. Calabria, A.R., Weidenfeller, C., Jones, A.R., de Vries, H.E. & Shusta, E.V. Puromycin-purified rat brain microvascular endothelial cell cultures exhibit improved barrier properties in response to glucocorticoid induction. *Journal of neurochemistry* **97**, 922-933 (2006).
6. Verbeek, M.M., Otte-Holler, I., Wesseling, P., Ruiter, D.J. & de Waal, R.M. Induction of alpha-smooth muscle actin expression in cultured human brain pericytes by transforming growth factor-beta 1. *The American journal of pathology* **144**, 372-382 (1994).